Is Turbulence a State of Maximal Dissipation?

Martin Mihelich, Davide Faranda, Didier Paillard, Bérengère Dubrulle

MDPI

Article

Is Turbulence a State of Maximum Energy Dissipation?

Martin Mihelich [1,†], Davide Faranda [2], Didier Paillard[2] and Bérengère Dubrulle [1,*]

[1] SPEC, CEA, CNRS, Université Paris-Saclay, CEA Saclay 91191 Gif sur Yvette cedex, France
[2] LSCE-IPSL, CEA Saclay l'Orme des Merisiers, CNRS UMR 8212 CEA-CNRS-UVSQ, Université Paris-Saclay, 91191 Gif-sur-Yvette, France

* Correspondence: berengere.dubrulle@cea.fr; Tel.: +33-169 087 247

† Current address: ma.mihelich@gmail.com

Academic Editor: name

Version March 22, 2017 submitted to Entropy

Abstract: Turbulent flows are known to enhance turbulent transport. It has then even been suggested that turbulence is a state of *maximum energy dissipation*. In this paper, we re-examine critically this suggestion at the light of several recent works around the Maximum Entropy Production principle (MEP) that has been used in several out-of-equilibrium systems. We provide a set of 4 different optimization principles, based on maximization of energy dissipation, entropy production, Kolmogorov-Sinai entropy and minimization of mixing time, and study the connection between these principles using simple out-of-equilibrium models describing mixing of a scalar quantity. We find that there is a chained-relationship between most probable stationary states of the system, and their ability to obey one of the 4 principle. This provides an empirical justification of the Maximum Entropy Production principle in this class of systems, including some turbulent flows, for special boundary conditions. Otherwise, we claim that the minimization of the mixing time would be a more appropriate principle. We stress that this principle might actually be limited to flows where symmetry or dynamics impose pure mixing of a quantity (like angular momentum, momentum or temperature). The claim that turbulence is a state of maximum energy dissipation, a quantity intimately related to entropy production, is therefore limited to special situations that nevertheless include classical systems such as Shear flows, Rayleigh Benard convection and von Karman flows, forced with constant velocity or temperature conditions.

Keywords: Maximum Entropy Production; Turbulence; Kolmogorov-Sinai entropy

1. Introduction: Turbulence as a maximum Energy Dissipation State?

A well-known feature of any turbulent flow is the Kolmogorov-Richardson cascade by which energy is transferred from scale to scale until scales at which it can be dissipated. This cascade is a non-linear, non-equilibrium process. It is believed to be the origin of the significant enhancement of dissipation observed in turbulent flow, often characterized via the introduction of a *turbulent viscosity*.

It has then sometimes been suggested that turbulence is a state of *maximum energy dissipation*. This principle inspired early works by Malkus [1,2] or Spiegel [3] to compute analytically the heat or momentum profiles in thermal boundary layers or linear shear flows. While there were many

criticisms about this principle, there are a few experimental situation where this principle seems to work. A good example is provided by the von Karman flow. This flow is generated by two-counter rotating impellers inside a cylindrical vessel filled e.g. with water (see Figure 1). The impellers produce a source of angular momentum at the top and bottom of the vessel, angular momentum that is then transferred and mixed within the flow throughout the turbulent motions [4], in analogy with heat transferred through a Rayleigh-Benard cell. For most impellers, the resulting mean large scale stationary motion is the superposition of a two-cell azimuthal motion, and a two cell poloidal motion bringing the flow from the top and bottom end of the experiment towards its center plane $z = 0$ (see Figure 1). This mean flow is thus symmetrical with respect to the plane $z = 0$. For some types of impellers, however, this symmetrical state is unstable, and bifurcates after a certain time towards another state that breaks the system symmetry [5,6]-see Figure 2. This state corresponds to a global rotation in the direction of either the top or the bottom impeller. The energy dissipation corresponding to either one of these 3 states can be measured through monitoring of the torque applied to the impellers by the flow. When monitored during a bifurcation (see Figure3), this energy dissipation displays a jump (by a factor 4) at the moment of the bifurcation from the symmetrical state towards either one of the non-symmetrical states. Once the system is in the bifurcated state, it never bifurcates back towards the symmetrical state, indicating that the most stable state is the state with larger dissipation.

This observation is in agreement with a general principle inspired from Malkus principle, that could be formulated as follow:

Principle A: In certain non-equilibrium systems with coexistence of several stationary state, the most stable one is that of Maximum Energy Dissipation.

This principle is of course very appealing. There are however no derivation of it from any first principles, and we are not aware of any theories that could lead to its proof (while there are probably many immediate counter-example that can be provided). If it is true or approximately true for some types of flows (like the von Karman flow, or the Rayleigh-Benard flow or the plane Couette flow), it may then lead to interesting applications allowing the computation of mean velocity or temperature profile without the need to integrate the whole Navier-Stokes equations. A way to proceed with its justification is to transform it into an equivalent principle, that uses notions more rooted in non-equilibrium physics. Indeed, energy dissipation is not a handful quantity to work with in general, because of its dependence on the small scale processes that produce it. In general, energy dissipation is a signature of entropy production. The connection between energy dissipation and entropy production was heuristically made by Lorenz [7] and theoretically discussed in nonlinear chemical thermodynamics by Dewar [8] and Moroz [9,10]. This last notion seems more appealing to work with and a first natural step is to modify slightly the principle A into a more appealing version as:

Principle B: In certain non-equilibrium systems with coexistence of several stationary state, the most stable one is that of Maximum Entropy Production (MEP).

From the point of view of non-equilibrium physics, this principle appears as a counterpart of the well known principle of Maximum Entropy that governs stability of equilibria in statistical physics, the analog of equilibria here being the stationary states. This principle was discovered by Ziegler [11,12] and it is sometimes referred to as the Ziegler's principle. It has found several applications in climate dynamics: first it was used by Paltridge [13] to derive a good approximation of the mean temperature distribution in the mean atmosphere of the Earth. This approach has been extend to more exhaustive climate models by Herbert [14]. Kleidon et al. [15] used an atmospheric general circulation model to show that MEP states can be used as a criterion to determine the boundary layer friction coefficients.

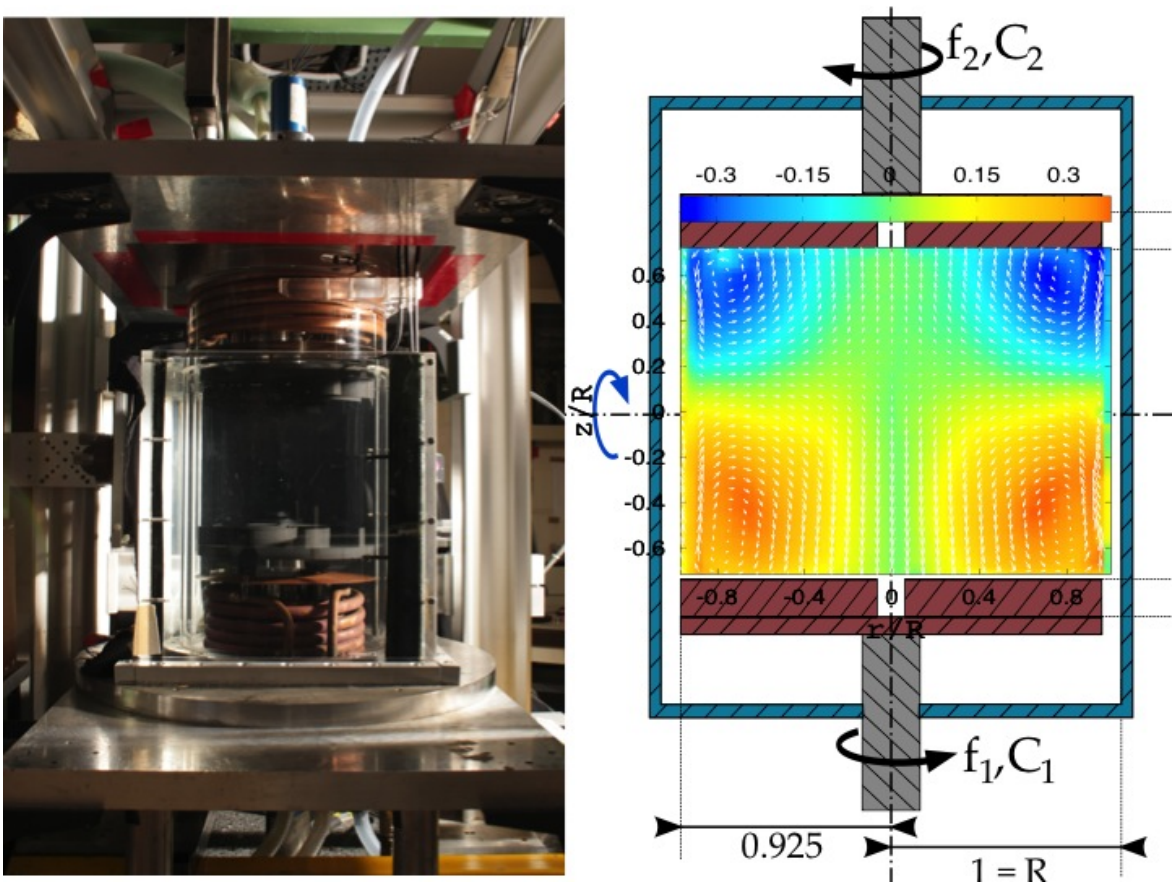

Figure 1. Von Karman experiment. The flow is generated inside a cylindrical vessel through counter-rotation of two impellers. The impellers inject angular-momentum at the top and the bottom, inducing a large scale circulation inside the flow. At low Reynolds numbers, the circulation is symmetrical with respect to a π-rotation around a horizontal axis through the origin (blue arrow). One can impose the torque C_i or the rotation frequency f_i to the flow, generating different turbulent regimes. The right picture shows a representation of the mean velocity fields in a plane passing for the axis of the cylinder (arrows) and orthogonal to this plane (colorscale in m/s), obtained by averaging several thousands instantaneous fields. (Pictures courtesy Brice Saint-Michel).

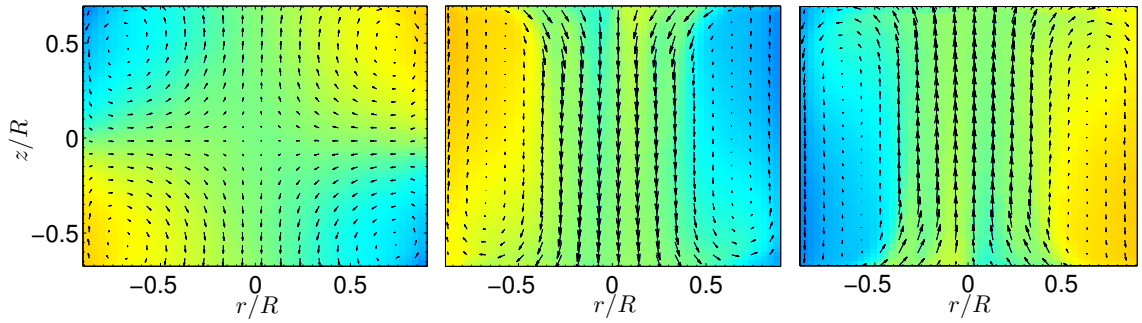

Figure 2. The 3 stationary states of the von Karman flow: left: The symmetric state. Middle and right: the two bifurcated states, that are symmetric to each other with respect to a π-rotation along an axis going through the rotation axis [5,6]. Color coding as in Figure 1.

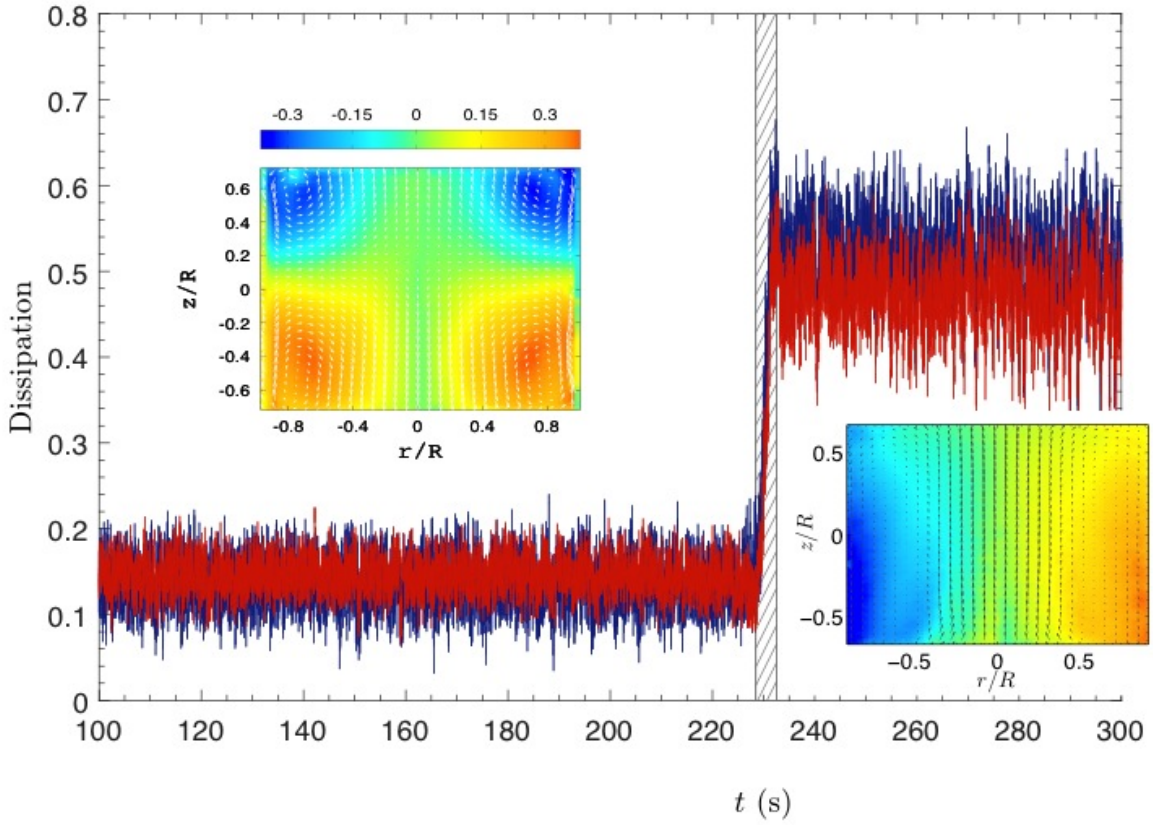

Figure 3. Spontaneous bifurcation in the von Karman flow: the flow, initially started in a symmetrical state, bifurcates after a certain time toward a bifurcated state, that produces a 4 times larger dissipation [5]. The dissipation is measured through monitoring of the torque, applied on each propeller, by the turbulent flow. This flow being turbulent, the resulting torque is widely fluctuating around a mean value, characterizing the dissipation. Color coding of the flow as in Figure 1. Colour coding of the dissipation is blue for the dissipation measured on the lower propeller, and red for the dissipation measured on the upper-propeller. The total dissipation is the some of the two contributions.

MEP seems also a valuable principle to describe planetary atmospheres, as those of Mars and Titan where it has been used to determine latitudinal temperature gradients [16]. MEP have been also applied to several geophysical problems: to describe thermally driven winds [17] and convection[18], and to oceanic circulation [19]. A detailed overview on the usefulness of MEP in climate science can be found in [20,21] and references therein. It is therefore interesting to evaluate the soundness of this principle and understand its limitation and its possible improvements, to extend as possible the scope of its applications. The usual path to prove the validity of a principle is to provide some rigorous demonstration of the principle itself. This task has been attempted without convincing results in the past years [8,22,23]. In the absence of any theory of out-of-equilibrium systems, we may turn to equilibrium theory as a guide to find a path for justification of the selection of stationary states. In equilibrium systems or conceptual models, this selection can be studied using the dynamical systems theory, where other quantities than thermodynamics entropy are relevant. One of this quantity is the Kolmogorov Sinai Entropy (KSE) [24], which is indeed different from the thermodynamic one. The KSE appears a good candidate for the selection of preferred metastable states because it is related to the concept of mixing time [25]. The goal of this paper is therefore to show that MEP principle could find a justification in a linked relationship which involves studying the connections among MEP, KSE and mixing times. The paper follow this structure: after discussing the relation between MEP and the Prigogine minimization principle (section II), we connect MEP and maximum KSE in conceptual models of turbulence (section III). In section IV we establish the link between maximum KSE and mixing times for Markov chains. Then, we summarize the results and discuss the implications of our findings.

2. Maximization or Minimization of Entropy production?

At first sight, Principle B appears in conflict with an established result of Prigogine, according to which the stationary states of a system close to equilibrium are states with *minimum* entropy production. In fact, both principles can be reconciled if Principle B is viewed as a MaxMin, principle: Martyushev et al. [26] and Kleidon [21] suggest that Prigogine's principle select the steady state of minimum entropy production compared to transient states. For a steady-state condition, the minimum entropy production principle does not give any further information if many steady state conditions are possible given the imposed boundary conditions. To provide a simple example, let us consider a system characterized by two parameters, T and U, where T controls the departure from equilibrium and U labels an additional constraint of the system, allowing the existence of several stationary states at a given T (see Figure 4). In our von Karman system, T could for example label the velocity fluctuations, and U the angular momentum transport. In the T direction, application of the Prigogine principle selects the value of T corresponding to the stationary state. When there are several possible stationary state, the Principle B then selects the most stable state as the one with the largest entropy production, thereby fixing the corresponding value of U. This was precisely the procedure followed by Paltridge.

On the other hand, it appears that the stability of the stationary state may depend on boundary conditions. For example, Niven [27] or Kawazura and Yoshida [28] provide explicit examples of out-of-equilibrium systems, in which the entropy production is sl maximized for fixed temperature boundary conditions, while it is *minimized for fixed heat flux* boundary conditions. In the experimental von Karman system discussed in Section 1, we observe a similar phenomenon: for fixed propeller velocities, the selected stationary state is the one of maximum dissipation. However, when one changes the boundary conditions into fixed applied torque at each propeller, the stationary state regime disappears and is replaced by a dynamical regime, in which the system switches between different meta-stable states of low and high energy dissipation [6]. This case is discussed in more detail in Section 6. It shows however that we cannot trust the Maximum Entropy Production principle blindly, and must find ways to understand why and when it works, using tools borrowed from

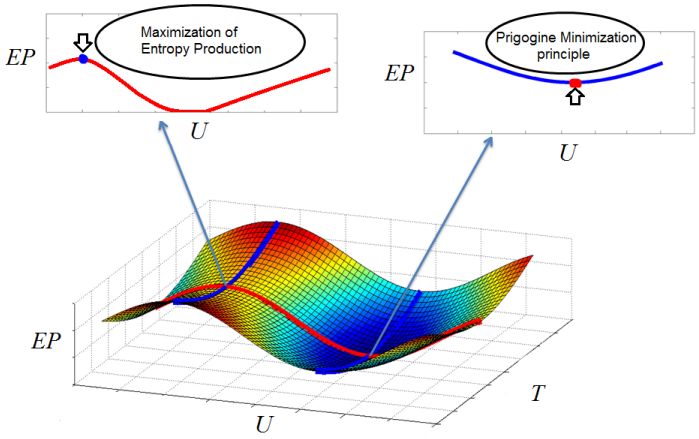

Figure 4. Illustration of the relation between maximization of entropy production EP and Prigogine principle: the system is set out of equilibrium by the parameters T and U. T controls the departure from equilibrium and U labels an additional constraint of the system. In the T direction, application of the Prigogine principle selects the value of T corresponding to the stationary state, where MEP selects the one with largest EP in the U direction.

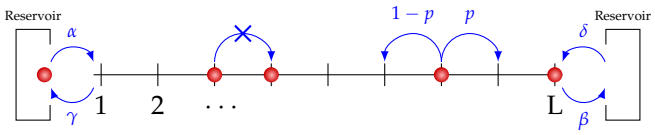

Figure 5. The dynamical rules of the toy model of scalar transport: the particle can jump to the left or to the right with probabilities denied by p. At both end, two reservoirs sets the flux of incoming or outgoing particles. The particle can be a boson (several particles per box are allowed), in which case the process is called zero-range process (ZRP). When the particle is a fermion, jump towards a box that is already occupied are forbidden. The corresponding process is called asymmetric exclusion process (ASEP).

non-equilibrium theories. A justification has been attempted [8], and dismissed [22,23], following the ideas of Jaynes that non-equilibrium systems should be characterized by a probability distribution on the trajectories in phase space, instead of just the points in phase space at equilibrium. A more pragmatic way to evaluate the validity of Principle B is to consider its application to toy models of non-equilibrium statistics, that mimics the main processes at work in the von Karman flow, and that can guide us on a way to a justification (or dismissal). This is the topic of the next section.

3. From Maximum entropy production to Maximum Kolmogorov-Sinai entropy in toy models of turbulence

3.1. From passive scalar equation to Markovian box models

In the von Karman flow, angular momentum is transported from the vessel ends towards the center. In Rayleigh-Benard, the temperature is transported from the bottom to the top plates. In shear flows, the linear momentum is transported from one side to the other. On Earth, the heat is transported from the equator towards the pole. All this system in which Principle B seems to provide a non-trivial answer have then in common that they deal with the transport of a scalar quantity T by a given velocity field $u(x,t)$, and that may be sketched as:

$$\partial_t T + u\nabla T = \kappa(\nabla)^2 T, \tag{1}$$

with appropriate boundary conditions. Here κ is the diffusivity. To transform this process into a tractable toy model, we stick to a one dimensional case and divide the accessible space ℓ into L boxes. We impose the boundary conditions through two reservoirs located at each end of the chain (mimicking e.g. the top and bottom propeller or solar heat flux at pole and equator). The boxes contains bosonic or fermionic particles that can jump in between two adjacent boxes via decorrelated jumps (to the right or to the left) following a 1D Markov dynamics governed by a coupling with the two reservoirs imposing a difference of chemical potential at the ends. The different jumps are described as follow. At each time step a particle can jump right with probability pw_n or jump left with probability $(1-p)w_n$. w_n is a parameter depending on the number of particles inside the box and on the nature of particles. Choices of different w_n give radically different behaviors. For fermionic particles, it prevents a jump on to a site, if this site is already occupied by a particle. The corresponding process is called Asymmetric Exclusion Process (ASEP). For boson, $w_n = 1$ and the process is called Zero Range Process (ZRP). At the edges of the lattice the probability rules are different: at the left edge a particle can enter with probability α and exit with probability γw_n whereas at the right edge a particle can exit with probability βw_n and enter with probability δ.

Without loss of generality, we may consider only $p \geq 1/2$ which corresponds to a particle flow from the left to the right and note $U = 2p - 1$. After a sufficiently long time the system reaches a non-equilibrium steady state, with a well defined density profile (or fugacity profile) across the boxes ranging between ρ_a, the density of the left reservoir and ρ_b, the density of the right reservoir, given by $\rho_a = \alpha(\gamma + \epsilon\alpha)$ and $\rho_b = \delta(\beta + \epsilon\delta)$, where $\epsilon = 1$ for ASEP (fermion) and $\epsilon = -1$ for ZRP (boson). In the sequel, we fix $\gamma + \alpha = 1$ and $\beta + \delta = 1$, and denote $\Delta T = \rho_a - \rho_b$ the parameter that measures the balance between the input rate of the left reservoir (the equivalent of the heat or momentum injection), and the removal rate of the right reservoir (the equivalent of the heat or momentum dissipation). Once β (say), ΔT are fixed, we can compute all the other parameter α, γ and δ of the model. In the sequel, we fix $\beta = 0.75$, and vary ΔT and/or U.

Taking the continuous limit of this process, it may be checked that the fugacity $Z = \rho/(1+\rho)$ of stationary solutions of a system consisting of boxes of size $\frac{1}{L}$ follow the continuous equation [29]:

$$U\frac{\partial Z}{\partial x} - \frac{1}{2L}\frac{\partial^2 Z}{\partial x^2} = 0, \tag{2}$$

corresponding to stationary solution of a passive scalar equation with velocity U and diffusivity $\frac{1}{2L}$. Therefore, the fugacity Z is a passive scalar obeying a convective-diffusion equation. We thus see that $U = 0$ corresponds to a purely conductive regime whereas the larger U the more convective the regime. This toy model therefore mimics in the continuous limit the behavior of scalar transport in the von Karman, Rayleigh-Bénard, Couette or Earth system we are trying to understand. The toy model is a discrete Markov process with 2^L states. It is characterized by its transition matrix $P = (p_{ij})$ which is irreducible. Thus, the probability measure on the states converges to the stationary probability measure $\mu = (\mu_{1_{stat}}, ..., \mu_{2^L_{stat}})$ which satisfies:

$$\mu_{i_{stat}} = \sum_{j=1}^{2^L} \mu_{j_{stat}}.p_{ji} \; \forall i \in [\![1, 2^L]\!]. \tag{3}$$

This Markov property makes our model simple enough so that exact computations are analytically tractable and numerical simulations are possible up to $L = 10$ (ASEP model) to $L = 1000$ (ZRP model) on a laptop computer. The idea now is to apply the Principle B in these toy models, and see what useful information we can derive from it.

3.2. Maximum Entropy production in Zero Range and ASymmetric Exclusion Process

We turn to the definition of entropy production in our toy model system. For a macroscopic system subject to thermodynamic forces X_i and fluxes J_i, the thermodynamic entropy production is given by: [30,31]:

$$\sigma_{thermo} = \sum_i J_i X_i \tag{4}$$

The fluxes to consider for a diffusive particles model are fluxes of particles and the thermodynamic forces can be written $X = \Delta(-\frac{\nu}{T})$ where T is the temperature and ν the chemical potential proportional to $\log(\rho)$ for an ideal gas [30]. So, as the temperature is here fixed, the thermodynamic Entropy production of a given stationary state takes the form:

$$\sigma_{thermo} \propto \sum_{i=1}^{L} J_i.(\log(\rho_i) - \log(\rho_{i+1})) = J.(\log(\rho_1) - \log(\rho_L)) \tag{5}$$

where ρ is the stationary density distribution and $J = J_i$ the particle fluxes in the stationary state, where all fluxes become equal and independent on the site. ρ and J are both (nonlinear) function of U. It is easy to show [32] that this definition is just the continuous limit of the classical thermodynamic entropy production in an ideal gas, that reads:

$$\sigma_{thermo} = -\int_{A_+}^{B_-} J(x,t) \frac{\partial \log(\rho(x,t))}{\partial x} dx \tag{6}$$

In the case of bosonic particles (ZRP model), this entropy production takes an compact analytical shape in the (thermodynamic) limit $L \to 0$ [33]:

$$\sigma(U) = \frac{\alpha U}{U+\gamma}(\log(\frac{\alpha}{U+\gamma-\alpha}) - \log(\frac{(\alpha+\delta)U+\gamma\delta}{U(\beta-\alpha-\delta)+\beta\gamma-\gamma\delta})) \tag{7}$$

Because $U = 2p - 1 \geq 0$ the entropy production is positive if and only if $\rho_a \leq \rho_b$. This means that fluxes are in the opposite direction of the gradient. We remark than if $U = 0$ then $\sigma(U) = 0$. Indeed J is proportional to U in this model. Moreover, $\sigma(U)$ is zero also when $\rho_1 = \rho_L$. This happens when U increases, $\rho_a(U)$ decreases and $\rho_b(U)$ increases till they take the same value. Thus it exists U, large enough, for which $\sigma(U) = 0$. Between these two values of U the entropy production has at least one maximum. By computing numerically the entropy production, we observe in fact that it is also true for the fermionic particles, even though we cannot prove it analytically. This is illustrated in Figure 6 for $L = 100$ (ZRP) and $L = 10$ (ASEP).

The value of $U_{max_{EP}}(T)$ at which this maximum occurs depends on the distance to equilibrium of the system, characterized by the parameter $\Delta T = \alpha - \delta$. In the case of the ZRP model, it can be computed as [33]:

$$U_{max_{EP,ZRP}} = \frac{\Delta T}{4M\alpha} + 3\frac{\Delta T^2(\alpha+1)}{8M^2\alpha^2(\alpha-1)} + o((\Delta T)^2), \tag{8}$$

where $M = (1+2\rho_a)(1+2\rho_b)$. This means that at equilibrium ($\Delta T = 0$, $\rho_a = \rho_b$), the maximum is attained for $U = 0$, i.e. the symmetric case. Numerical simulations of the ASEP system suggest that this behavior is qualitatively valid also for fermionic particles: the entropy production displays a maximum, that varies linearly in ΔT . Such behavior therefore appears quite generic of this class of toy model. When the system is close to equilibrium ($\Delta T \ll 1$), the maximum is very near zero, and, the density profile is linear, corresponding to a *conductive* case. When the system is out-of-equilibrium ($\Delta T \geq 0$) the maximum is shifted towards larger values of $U > 0$, corresponding to a *convective state*, with flattened profile. An example is provided in Figure 7 for the ZRP and ASEP model.

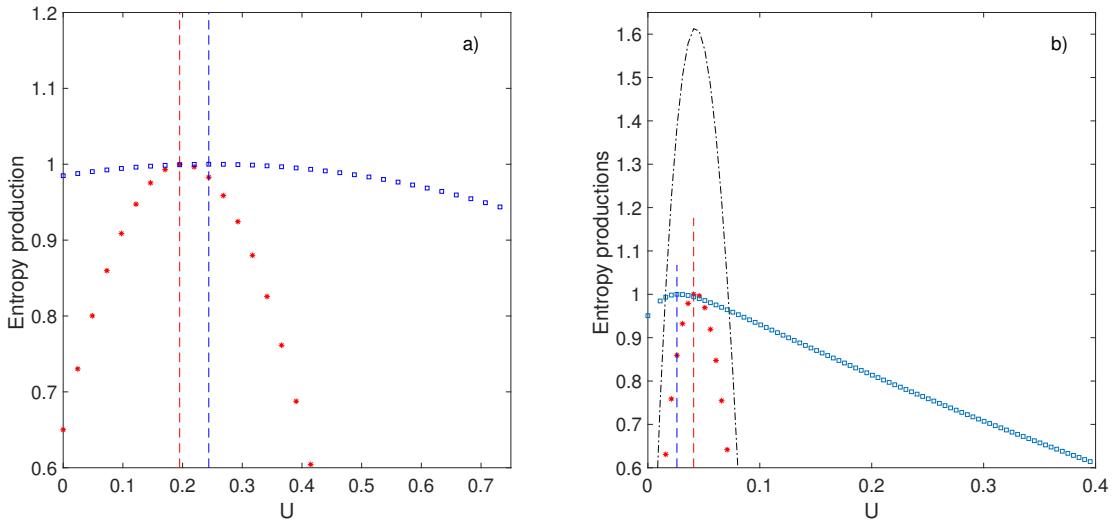

Figure 6. Entropy productions as a function of U for $\beta = 0.75$ and $\Delta T = 0.25$ for two toys models. Red stars: Thermodynamic entropy production $\sigma(U)$; blue squares: Kolmogorov-Sinai entropy $h_{KS}(U)$. The location of the maxima are denoted by vertical dashed line (red for $\sigma(U)$; and blue for $h_{KS}(U)$). a) Case L=10 ASEP (fermion) ; b) Case L=100 ZRP (boson) . The dot-dashed line is the asymptotic law for $\sigma(U)$ given by Eq. (7).

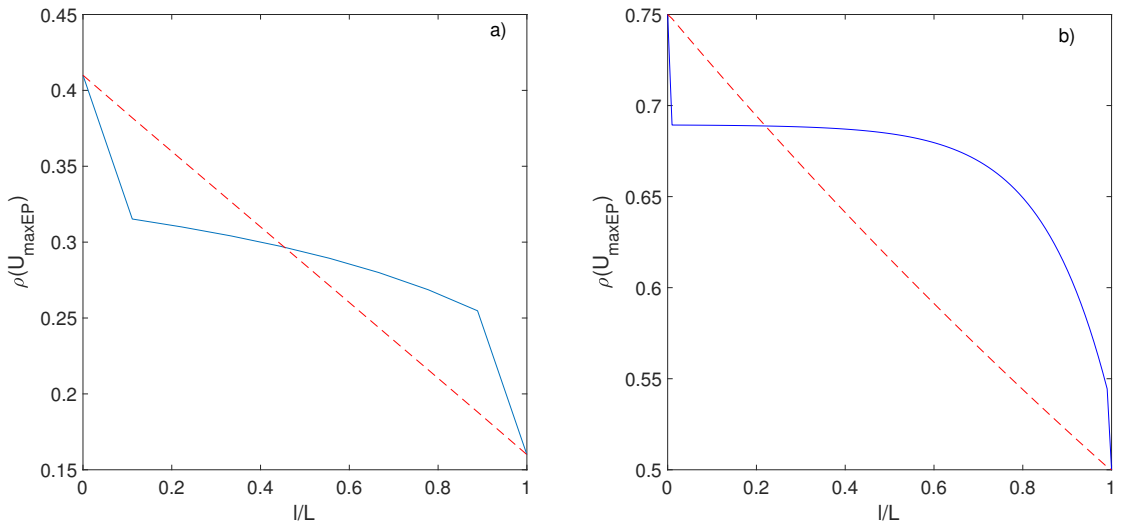

Figure 7. Profiles of density profiles (blue line) corresponding to models with $U = U_{maxEP}$ for $\beta = 0.75$ and $\Delta T = 0.25$ for two toys models. The red dashed line is the density profile obtained at $U = 0$, i.e. in the *conductive case*. a) Case L=10 ASEP (fermion) ; b) Case L=100 ZRP (boson)

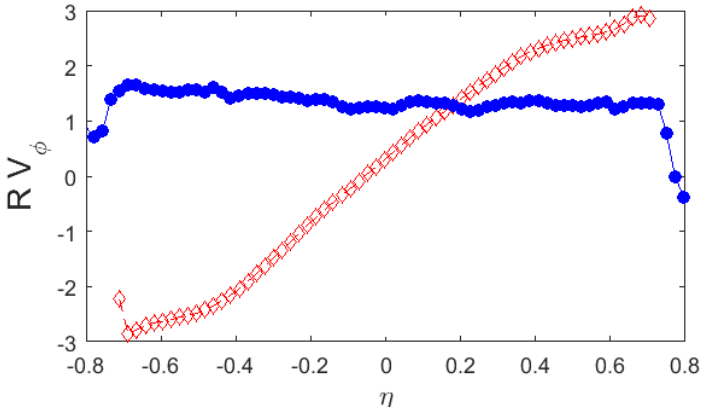

Figure 8. Profiles of angular momentum RV_ϕ as a function of the height from the central plane η in the von Karman laboratory experiment. Blue symbols with line: in the *bifurcated* state with higher energy dissipation. Red line with symbols: in the symmetric state.

Our toy models are examples of systems with deviation from equilibrium (labelled by ΔT), admitting several stationary states (labelled by U). So if we were to apply our MinMax/Principle B to these toy models, we would select the model corresponding to $U_{max_{EP}}$ as the most stable one, i.e. the conductive state with linear profile at equilibrium, and the convective state with flattened profile at non-equilibrium. Interestingly enough, this selection corresponds qualitatively to the type of profiles that are selected by the non-linear dynamics in the von Karman, Rayleigh-Benard or Couette system, as illustrated in Figure 8 for the VK flow: for low levels of fluctuations (low Reynolds or impeller with moderately bent blades) corresponding to close to equilibrium state, the most stable state is the symmetric state, with linear angular momentum profile. At larger fluctuation rates, the most stable state is the bifurcated state, with flat angular momentum at the center.

The ability of Principle B, based only on entropy i.e. *equilibrium* notions, to predict at least qualitatively the correct behavior of scalar transport in several non-equilibrium turbulent system is puzzling. It would be more satisfying to connect this Principle to other notions that seem more appropriate in the case of non-equilibrium system. This is the topic of the next section.

3.3. From Maximum Entropy Production to Kolmogorov-Sinai Entropy

The physical meaning of the thermodynamic entropy production is the measure of irreversibility: the larger σ the more irreversible the system [34] . It is however only a *static* quantity, being unconnected to the behavior of trajectories in the phase space. In that respect, it is not in agreement with the ideas of Jaynes that non-equilibrium systems should be characterized by a probability distribution on the trajectories in phase space, instead of just the points in phase space at equilibrium. In the context of Markov chains, Jaynes' idea provides a natural generalization of equilibrium statistical mechanics [35], by considering the Kolmogorov-Sinai entropy (KSE). There are many ways to estimate the Kolmogorov-Sinai entropy associated with a Markov chain [35,36].The most useful one in our context is the one defined as the time derivative of the Jaynes entropy. To characterize the dynamics of the system during the time interval $[0, t]$, one considers the possible dynamical trajectories $\Gamma_{[0,t]}$ and the associated probabilities $p_{\Gamma_{[0,t]}}$. The dynamical trajectories entropy- the Jaynes entropy- reads:

$$S_{Jaynes}(t) = -\sum_{\Gamma_{[0,t]}} p_{\Gamma_{[0,t]}} . \log(p_{\Gamma_{[0,t]}}) \tag{9}$$

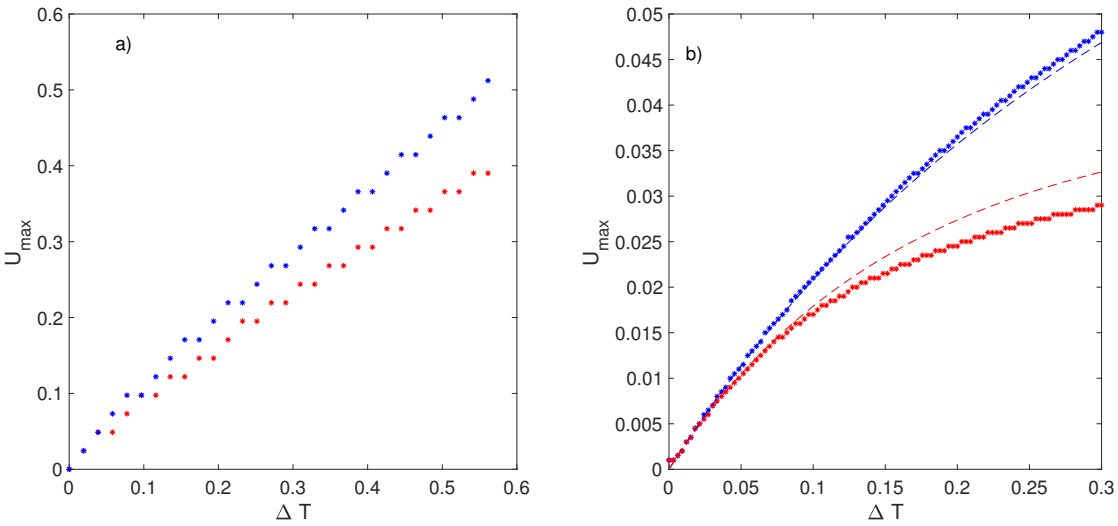

Figure 9. Location of the maximum of thermodynamic entropy production U_{maxEP} (red stars) and maxim of Kolmogorov-Sinai entropy (blue stars) as a function of ΔT. a) Case L=10 ASEP (fermion). b) Case L=100 ZRP (boson). The red dashed line is the second order approximation given by Eq. (8). The blue-dashed line is the first order approximation to the location of the maxima (Eq. (12)).

For a Markov chain we find that:

$$S_{Jaynes}(t) - S_{Jaynes}(t-1) = -\sum_{(i,j)} \mu_{i_{stat}} p_{ij} \log(p_{ij}) \tag{10}$$

Thus, the Kolmogorov-Sinai Entropy for the Markov chain is:

$$h_{KS} = -\sum_{(i,j)} \mu_{i_{stat}} p_{ij} \log(p_{ij}), \tag{11}$$

where μ_i is the stationary measure and p_{ij} the transition matrix.

In the case of bosonic particles (ZRP model), the KSE can be computed analytically and it admits a maximum as a function of U [33]. The value of U corresponding to this maximum can also be computed analytically, and leads to:

$$U_{max_{KS}} = \frac{\Delta T}{4M\alpha} + o(\Delta T), \tag{12}$$

Such first order approximation appear to be valid even far from equilibrium (see Figure 9). Comparing with the value for the maximum of entropy production, we see that the two maxima coincide, to first order in ΔT and $1/L$: in the continuous limit, Principle B provides the same kind of information than a third principle that we may state as:

Principle C: In certain non-equilibrium systems with coexistence of several stationary state, the most stable one is that of Maximum Kolmogorov-Sinai Entropy.

Is this third principle any better that the principle B? In our toy models, it seems to give the same information than the Principle B: for ZRP, we have shown analytically that the maxima of each principle coincide to first order in ΔT and $1/L$. Numerical simulation of the ASEP system suggests that it is also true for fermionic particles: for a given value of ΔT the difference between the two maxima $\Delta U_{max} = U_{max_{EP}} - U_{max_{KS}}$ decreases with increasing L [32]. For a fixed L, the difference

between the two maxima increases with ΔT, but never exceeds a few percent at $L = 10$ [32], see Figure 9).

In turbulent system, the test of this principle is more elaborate, because the computation of h_{KS} is not straightforward. It would however be interesting to test it in numerical simulations.

4. From Maximum Kolmogorov-Sinai entropy to Minimum Mixing Time in Markov Chains

Principle C is appealing because it involves a quantity clearly connected with dynamics in the phase space, but it is still unclear why the maximization of the entropy associated with paths in the phase space should select the most stable stationary state, if any. To make such a link, we need to somehow connect to the relaxation towards a stationary state, i.e. the time a system takes to reach its stationary state. In Markov chains, such a time is well defined, and is called the mixing time. Intuitively, one may think that the smaller the mixing time, the most probable it is to observe a given stationary state. So there should be a link between the maximum of Kolmogorov-Sinai entropy, and the Minimum mixing time. This link has been derived in [25], for general Markov chains defined by their adjacency matrix A and transition matrix P, defined as follows: $A(i,j) = 1$ if and only if there is a link between the nodes i and j and 0 otherwise. $P = (p_{ij})$ where p_{ij} is the probability for a particle in i to hop on the j node. Specifically, it has been shown that Kolmogorov-Sinai entropy increases with decreasing mixing time (see Figure 1 in [25]). More generally, for a given degree of sparseness of the matrix A (number of 0), the Markov process maximizing the Kolmogorov-Sinai entropy is close (using an appropriate distance) to the Markov process minimizing the mixing time. The degree of closeness depends on the sparseness, and becomes very large with decreasing sparseness, i.e. for unconstrained dynamics (Figure 3 in [25]).

This result provides us with a fourth principle in Markov chains:

Principle D: In certain non-equilibrium systems with coexistence of several stationary states, the most stable one is that of Minimum Mixing Time.

Given what we have seen before, there are 4 general principle that select the same stationary state, in the limit of large size and small deviations from out-of-equilibrium (see Figure 10). Among all 4, the Principle that provides the better understanding of its application is the Principle D, because the smaller the mixing time, the less time it is required to reach a given state and so the most probable the corresponding state. This phenomenological understanding can actually be given a deeper meaning when switching from Markov chains to Langevin systems.

5. From Minimum Mixing Time in Markov Chains to Mean Escape rate in Langevin systems

The notions we have derived in Markov chains have actually a natural counter-part in general Langevin systems. Consider indeed the general Langevin model:

$$\dot{x} = f(x) + \xi, \tag{13}$$

where $f(x)$ is the force and ξ is a delta-correlated Gaussian noise:

$$< \xi >= 0, \quad < \xi(t)\xi(t') >= 2D\delta(t - t'). \tag{14}$$

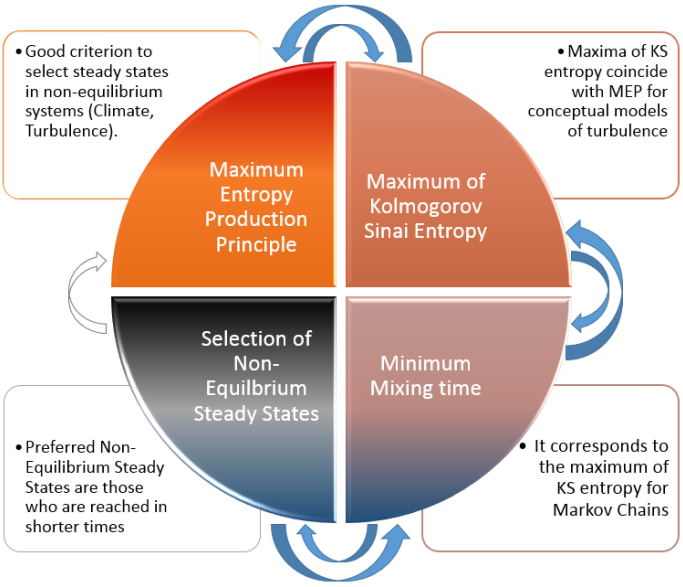

Figure 10. Conceptual path to demonstrate the validity of the Maximum Entropy Principle followed in this paper.

The probability distribution of x, $P(x,t)$ then obeys a Fokker-Planck equation:

$$\begin{aligned} \partial_t P(x,t) &= -\partial_x(f(x)P(x,t)) + D\partial_x\partial_x P(x,t), \\ &= \partial_x(J(x,t)P(x,t)), \end{aligned} \tag{15}$$

where $J = f(x)P(x,t) - D\partial_x P(x,t)$ is the current. It is well known (see e.g. [37]) that the discretization of the Langevin model on a lattice of grid spacing a (so that $x = na$) is a Markov chain, governed by the master equation:

$$\partial_t P_n = w^+_{n-1}P_{n-1} - w^+_n P_n + w^-_{n+1} - w^-_n P_n, \tag{16}$$

where P_n is the probability of having the particle at node n and $w^\pm_n$ are the probability of forward and backward jump at node n, given by:

$$\begin{aligned} w^+_n &= \frac{D}{a^2}, \\ w^-_n &= \frac{D}{a^2} - \frac{f_n}{a}. \end{aligned} \tag{17}$$

From this, we can compute the Kolomogorov-Sinai entropy as [38]

$$h_{KSL} =< w^+_n \ln \frac{w^+_n}{w^-_{n+1}} + w^-_n \ln \frac{w^-_n}{w^+_{n-1}} >, \tag{18}$$

which in the continuous limit $a \to 0$ becomes:

$$h_{KSLc} =< \frac{1}{D}|f(x)|^2 + f'(x) >, \tag{19}$$

which is the well know entropy production.

On the other hand, the dissipated power in the Langevin process can easily be computed as :

$$\mathcal{P} =< f\dot{x} >= \int J(x,t)f(x,t)dx =< |f|^2 + Df'(x) >= Dh_{KSLc}. \tag{20}$$

The Kolmogorov-Sinai entropy and the dissipated power are thus proportional to each other. In such example, it is thus clear that maxima of h_{KS} and maxima of entropy production coincide.

On the other hand, when f derives from a potential, $f = -\partial_x(U)$, there may be several meta-stable positions at U local minima. In such a case, it is known from diffusion maps theory and spectral clustering [39] that the exit times from the meta-stable states are connected to the smallest eigenvalues of the operator $\mathcal{H}$, such that $\mathcal{H}P = D\Delta P - \nabla P \nabla U$, which is the equivalent of the Liouville operator in Markov chain. More specifically, if U has N local minima, then the spectra of $\mathcal{H}$ has a cluster of N eigenvalues $\mu_1 < \mu_2 < .. < \mu_N$ located near 0, each of which being associated with the exit time it takes to get out from the local minima S_i to the state corresponding to the deepest minimum (the equilibrium state). For example, $\mu_1 = \frac{1}{\tau_1}$, where τ_1 is the mean exit time to jump the highest barrier of energy onto the deepest well. We see from that that the smaller the eigenvalue (equivalent to the mixing time), the longer time it takes to jump from this metastable state, and so the *more stable* is this state. This provides a quantitative justification of the notion that *the most stable stationary states* are the one with the minimum mixing time. It is worth mentioning that Langevin systems are now incorporated in numerical weather prediction to provide some flexibility to the sub-grid scales parameterizations [40]. Models based on these so-called stochastic parameterizations have usually better prediction skills than models based on deterministic parameterizations. Stochastic parameterization is therefore increasingly used in different aspects of weather and climate modeling [41]. We might speculate that, in these large simulations, the stochasticity helps models to reach more realistic results by favoring jumps to *more stable* states as outlined above. Another way to select these more realistic states could possibly be to search for the ones that maximize dissipation or entropy production, as was done empirically in a simple way in Paltridge's model [13,14].

6. Summary: Turbulence as a minimum Mixing Time State?

Considering a *mixing time* to characterize turbulence is natural, given the well known enhancement of mixing properties observed in turbulent flows. The mixing time defined for Markov chains is also comparable to the mixing time one would naturally define for turbulence, namely the smallest time after which a given partition of a scale quantity is uniformly spread over the volume. This time corresponds to the one defined by Arnold for dynamical systems [42] when introducing the concept of strong mixing. Here, it is the time associated with eigenvalues of the Liouville operator of the processes describing the turbulence action. In the specific example we consider here, namely von Karman flow, the turbulence is characterized by a symmetry along the rotation axis, which favors stationary states in which angular momentum is mixed along meridional planes [43,44].In this case, there is a clear connection between the equation obeying the angular momentum and the classical Fokker-Planck equation Eq. (15). One can thus hope in such a case to find a Langevin process describing the angular momentum mixing. This was actually done in [43] and shown to reproduce very well the power statistics in both regimes of constant torque and constant speed forcing, in case where there is only one stationary state. For multiple stationary states, obtained in the regime with fixed applied torque, the corresponding Langevin process has been derived in [45] and it turns out to be a non-linear stochastic oscillator, featuring multiple metastable states and limit cycles. Such oscillator is found to describe the dynamics of the reduced frequency $\theta = (f_1 - f_2)/(f_1 + f_2)$ which is a global observable respecting the symmetries of the flow. The challenge is then to compute the mixing times of the different metastable states arising in the non-linear stochastic oscillator.

In [46–48] we have shown that the mixing time τ of turbulent flows can be easily obtained by fitting the Langevin process (or aut-regressive process) $x_t = \phi x_{t-1} + \xi(t)$ to data. Here $x(t)$ is a global quantity tracing the symmetry of the flows, $\xi(t)$ is a random variable normally distributed and $-1 < \phi < 1$ is the so called auto-regressive coefficient. The link with the mixing time is made through the parameter $|\phi|$ which is indeed proportional to τ: the larger this quantity, the slower the mixing

in the system, because the dynamics weight more the present observation x_t when updating x_{t+1}. In [46], only flow configurations with a single stationary state have been analysed and ϕ computed using the complete time series. To extend the results to the flow regimes featuring multistability, we use the strategy outlined in [49]. First of all, we reconstruct the dynamics by using the embedding methodology on the series of partial maxima of θ, denoted as θ_i. A 2D section of the attractor is shown in the upper panel of Figure 11 and it is obtained by plotting θ_i as a function of the subsequent maxima θ_{i+1}. The histogram of θ_i is reported in the lower panel and show the correspondence to three metastable states s_1, s_2, s_3. Since we are not dealing with a stationary process, we cannot compute a single ϕ for the full time series of θ. The method introduced in [49] consists in computing a value of ϕ_i for each θ_i, taking the 50 previous observations of the complete time series. The distribution of $|\phi|$ is shown in colorscale in Figure 11. It is evident that the most represented states (s_1 and s_2) are those with the minimum mixing time whereas the most unstable one (s_3) is the one with the largest mixing time. This example shows that the results outlined in Section 5 can be extended to higher dimensions and that there is a simple strategy to compute the mixing times in complex systems.

It is quite plausible that such study can be generalized to turbulent systems with other symmetry, such as symmetry by translation along an axis. The turbulent shear flow enter in that category. Finally, we note that in Rayleigh-Bénard systems or in stratified turbulence, the temperature is also a quantity that is mixed within the flow, and that should also be liable to a Langevin description. It is therefore not a coincidence that shear flow, Rayleigh-Bénard convection and von Karman flows are so far the only systems in which the principle of Maximum Energy dissipation has been applied with some success. They are systems where a Langevin description is possible, and where the Maximum Energy dissipation principle in fact coincides with the Minimum Mixing time principle, connected to the longest exit time from meta-stable states. As observed by [50], these flows tends to be in a steady state with a distribution of eddies that produce the maximum rate of entropy increase in the nonequilibrium surroundings. In more general turbulence, it is not clear that such a Langevin description is possible, so that the statement of *Turbulence as a minimum Mixing Time State* might actually be limited to quite special situations, where symmetry or dynamics impose pure mixing of a quantity (like angular momentum, momentum or temperature). Shear flow, Rayleigh Benard convection and von Karman flows belong to this category.

Other conceptual pathways allow to link MEP to the underlying dynamics of the system: Moroz [51] suggests that the dissipation time minimization is linked to the least action principle, used in chemistry, biology and physics to derive the equations of motion. Although this theoretical formulation goes in the same direction of the results provided in this paper, our approach provides a rather practical way to connect dynamics and thermodynamics through statistical quantities directly computable from experimental time series.

Acknowledgments: M.M. and B.D. were supported by the ANR ECOUTURB. M.M. was supported by a fellowship from the LABEX PALM. DF was supported by ERC grant No. 338965

Author Contributions: M.M., B.D. and D.P. conceived and designed the models; B.D., D.F., and M.M. performed the numerical computations; M.M. B.D. and D.F. analyzed the data; all the authors wrote the paper.

Conflicts of Interest: The authors declare no conflict of interest.

Bibliography

1. Malkus, W.V. The heat transport and spectrum of thermal turbulence. Proceedings of the Royal Society of London A: Mathematical, Physical and Engineering Sciences. The Royal Society, 1954, Vol. 225, pp. 196–212.
2. Malkus, W. Outline of a theory of turbulent shear flow. *Journal of Fluid Mechanics* **1956**, *1*, 521–539.

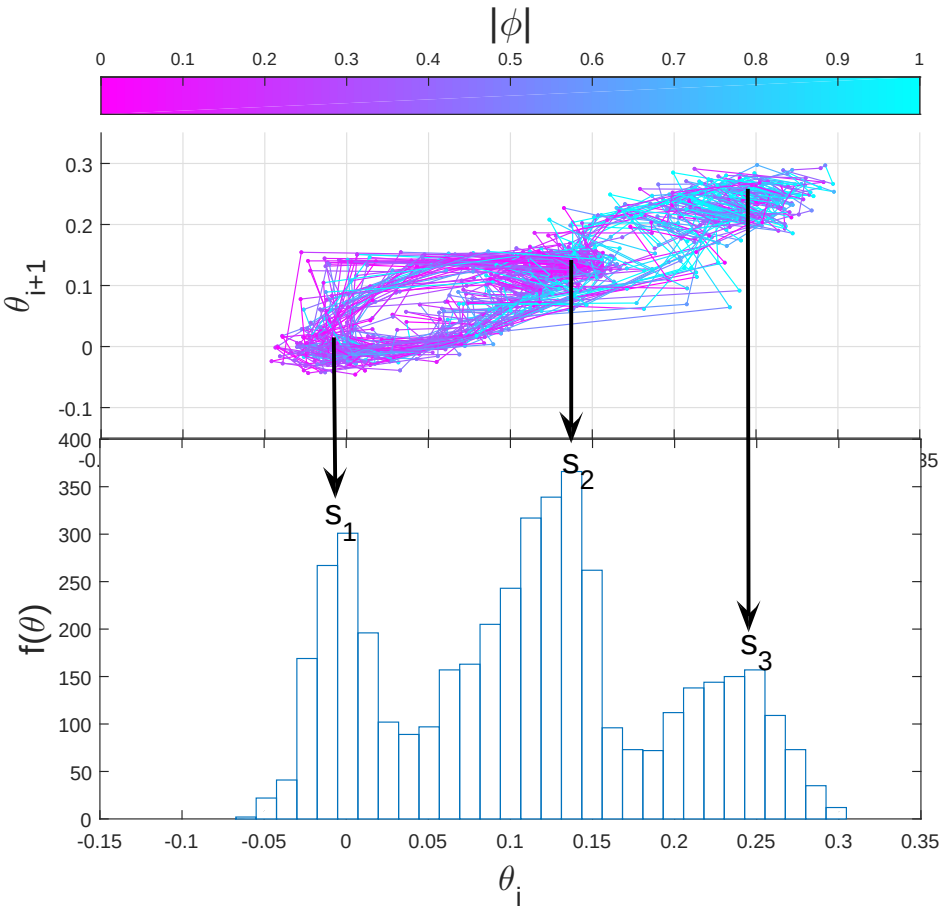

Figure 11. Upper panel: 2D Poincaré section of the Von Karman attractor obtained embedding the partial maxima of the reduced frequency θ_i. The colors represent $|\phi|$, the autoregressive coefficient computed for each of the θ_i, using the 50 previous observations of the full time series of θ. Lower panel: histogram of the partial maxima θ_i. The metastable state s_3 is visited less than s_1 and s_2 and corresponds to higher mixing time (values of $|\phi|$ close to 1)

3. Spiegel, E.A. Thermal turbulence at very small Prandtl number. *Journal of Geophysical Research* **1962**, *67*, 3063–3070.
4. Marie, L.; Daviaud, F. Experimental measurement of the scale-by-scale momentum transport budget in a turbulent shear flow. *Physics of Fluids (1994-present)* **2004**, *16*, 457–461.
5. Ravelet, F.; Marié, L.; Chiffaudel, A.; Daviaud, F. Multistability and memory effect in a highly turbulent flow: experimental evidence for a global bifurcation. *Physical review letters* **2004**, *93*, 164501.
6. Saint-Michel, B.; Dubrulle, B.; Marié, L.; Ravelet, F.; Daviaud, F. Evidence for forcing-dependent steady states in a turbulent swirling flow. *Physical review letters* **2013**, *111*, 234502.
7. Lorenz, E.N. Generation of available potential energy and the intensity of the general circulation **1960**.
8. Dewar, R.C. Information theory explanation of the fluctuation theorem, maximum entropy production and self-organized criticality in non-equilibrium stationary states. *J. Phys. A: Math. Gen.* **2003**, *36*, 631.
9. Moroz, A. On a variational formulation of the maximum energy dissipation principle for non-equilibrium chemical thermodynamics. *Chemical Physics Letters* **2008**, *457*, 448–452.
10. Moroz, A. A variational framework for nonlinear chemical thermodynamics employing the maximum energy dissipation principle. *The Journal of Physical Chemistry B* **2009**, *113*, 8086–8090.
11. Ziegler, H. Progress in Solid Mechanics, ed. IN Sneddon and R. Hill. *Amsterdam, The Netherlands: North-Holland Publishing Co* **1963**, *4*, 93.
12. Ziegler, H.; Wehrli, C. The derivation of constitutive relations from the free energy and the dissipation function. *Advances in applied mechanics* **1987**, *25*, 183–238.
13. Paltridge, G.W. Global dynamics and climate-a system of minimum entropy exchange. *Q. J. R. Meteorol. Soc.* **1975**, *101*, 475–484.
14. Herbert, C.; Paillard, D.; Kageyama, M.; Dubrulle, B. Present and Last Glacial Maximum climates as states of maximum entropy production. *Q. J. R. Meteorol. Soc.* **2011**, *137*, 1059–1069.
15. Kleidon, A.; Fraedrich, K.; Kunz, T.; Lunkeit, F. The atmospheric circulation and states of maximum entropy production. *Geophysical research letters* **2003**, *30*.
16. Lorenz, R.D.; Lunine, J.I.; Withers, P.G.; McKay, C.P. Titan, Mars and Earth: Entropy production by latitudinal heat transport. *Geophysical Research Letters* **2001**, *28*, 415–418.
17. Lorenz, R.D. Maximum frictional dissipation and the information entropy of windspeeds. *Journal of Non-Equilibrium Thermodynamics* **2002**, *27*, 229–238.
18. Ozawa, H.; Ohmura, A. Thermodynamics of a global-mean state of the atmosphere—a state of maximum entropy increase. *Journal of climate* **1997**, *10*, 441–445.
19. Shimokawa, S.; Ozawa, H. On the thermodynamics of the oceanic general circulation: Irreversible transition to a state with higher rate of entropy production. *Quarterly Journal of the Royal Meteorological Society* **2002**, *128*, 2115–2128.
20. Ozawa, H.; Ohmura, A.; Lorenz, R.D.; Pujol, T. The second law of thermodynamics and the global climate system: a review of the maximum entropy production principle. *Reviews of Geophysics* **2003**, *41*.
21. Kleidon, A. Nonequilibrium thermodynamics and maximum entropy production in the Earth system. *Naturwissenschaften* **2009**, *96*, 1–25.
22. Grinstein, G.; Linsker, R. Comments on a derivation and application of the 'maximum entropy production' principle. *J. Phys. A* **2007**, *40*, 9717–9720.
23. Bruers, S. A discussion on maximum entropy production and information theory. *J. Phys. A* **2007**, *40*, 7441–7450.
24. Gaspard, P.; Nicolis, G. Transport properties, Lyapunov exponents, and entropy per unit time. *Physical review letters* **1990**, *65*, 1693.
25. Mihelich, M.; Dubrulle, B.; Paillard, D.; Faranda, D.; Kral, Q. Maximum Kolmogorov-Sinai entropy vs minimum mixing time in Markov chains. *arXiv preprint arXiv:1506.08667* **2015**.
26. Martyushev, L.M.; Seleznev, V.D. Maximum entropy production principle in physics, chemistry and biology. *Phys. Rep.* **2006**, *426*, 1–45.
27. Niven, R.K. Simultaneous extrema in the entropy production for steady-state fluid flow in parallel pipes. *Journal of Non-Equilibrium Thermodynamics* **2010**, *35*, 347–378.
28. Kawazura, Y.; Yoshida, Z. Comparison of entropy production rates in two different types of self-organized flows: Bénard convection and zonal flow. *Physics of Plasmas* **2012**, *19*, 012305.

29. Levine, E.; Mukamel, D.; Schütz, G. Zero-range process with open boundaries. *Journal of statistical physics* **2005**, *120*, 759–778.
30. Balian, R. *Physique statistique et themodynamique hors équilibre*; Ecole Polytechnique, 1992.
31. De Groot, S.; Mazur, P. *Non-equilibrium thermodynamics*; Dover publications, 2011.
32. Mihelich, M.; Dubrulle, B.; Paillard, D.; Herbert, C. Maximum Entropy Production vs. Kolmogorov-Sinai Entropy in a Constrained ASEP Model. *Entropy* **2014**, *16*, 1037–1046.
33. Mihelich, M.; Faranda, D.; Dubrulle, B.; Paillard, D. Statistical optimization for passive scalar transport: maximum entropy production versus maximum Kolmogorov–Sinai entropy. *Nonlinear Processes in Geophysics* **2015**, *22*, 187–196.
34. Prigogine, I. *Thermodynamics of irreversible processes*; Thomas, 1955.
35. Monthus, C. Non-equilibrium steady states: maximization of the Shannon entropy associated with the distribution of dynamical trajectories in the presence of constraints. *J. Stat. Mech.* **2011**, p. P03008.
36. Billingsley, P. *Ergodic theory and information*; Wiley, 1965.
37. Tomé, T.; de Oliveira, M.J. Entropy production in irreversible systems described by a Fokker-Planck equation. *Physical Review E* **2010**, *82*, 021120.
38. Lebowitz, J.L.; Spohn, H. A Gallavotti–Cohen-type symmetry in the large deviation functional for stochastic dynamics. *Journal of Statistical Physics* **1999**, *95*, 333–365.
39. Nadler, B.; Lafon, S.; Coifman, R.R.; Kevrekidis, I.G. Diffusion maps, spectral clustering and eigenfunctions of Fokker-Planck operators. *arXiv preprint math/0506090* **2005**.
40. Palmer, T.N. A nonlinear dynamical perspective on model error: A proposal for non-local stochastic-dynamic parametrization in weather and climate prediction models. *Quarterly Journal of the Royal Meteorological Society* **2001**, *127*, 279–304.
41. Berner, J.; Achatz, U.; Batte, L.; Bengtsson, L.; De La Camara, A.; Christensen, H.M.; Colangeli, M.; Coleman, D.R.; Crommelin, D.; Dolaptchiev, S.I.; others. Stochastic parameterization: towards a new view of weather and climate models. *Bulletin of the American Meteorological Society* **2016**.
42. Arnold, V.I.; Avez, A. *Ergodic problems of classical mechanics*; Vol. 9, Benjamin, 1968.
43. Leprovost, N.; Marié, L.; Dubrulle, B. A stochastic model of torques in von Karman swirling flow. *The European Physical Journal B-Condensed Matter and Complex Systems* **2004**, *39*, 121–129.
44. Monchaux, R.; Cortet, P.P.; Chavanis, P.H.; Chiffaudel, A.; Daviaud, F.; Diribarne, P.; Dubrulle, B. Fluctuation-dissipation relations and statistical temperatures in a turbulent von Kármán flow. *Physical review letters* **2008**, *101*, 174502.
45. Faranda, D.; Sato, Y.; Saint-Michel, B.; Wiertel, C.; Padilla, V.; Dubrulle, B.; Daviaud, F. Stochastic chaos in a turbulent swirling flow. *arXiv preprint arXiv:1607.08409* **2016**.
46. Faranda, D.; Pons, F.M.E.; Dubrulle, B.; Daviaud, F.; Saint-Michel, B.; Herbert, É.; Cortet, P.P. Modelling and analysis of turbulent datasets using Auto Regressive Moving Average processes. *Physics of Fluids (1994-present)* **2014**, *26*, 105101.
47. Faranda, D.; Pons, F.M.E.; Giachino, E.; Vaienti, S.; Dubrulle, B. Early warnings indicators of financial crises via auto regressive moving average models. *Communications in Nonlinear Science and Numerical Simulation* **2015**, *29*, 233–239.
48. Faranda, D.; Defrance, D. A wavelet-based approach to detect climate change on the coherent and turbulent component of the atmospheric circulation. *Earth System Dynamics* **2016**, *7*, 517–523.
49. Nevo, G.; Vercauteren, N.; Kaiser, A.; Dubrulle, B.; Faranda, D. A statistical-mechanical approach to study the hydrodynamic stability of stably stratified atmospheric boundary layer **2016**.
50. Ozawa, H.; Shimokawa, S.; Sakuma, H. Thermodynamics of fluid turbulence: A unified approach to the maximum transport properties. *Physical Review E* **2001**, *64*, 026303.
51. Moroz, A. *The common extremalities in biology and physics: maximum energy dissipation principle in chemistry, biology, physics and evolution*; Elsevier, 2011.